



TDP43 LC (286-331) A315E	288-319	32	"R", kinked	4	2-fold screw	1	-1.3	4.81	1.2	10	cryoEM	3.3	Recombinant	-17.0	-0.53	6n3c
TDP43 LC (311-360) slow	311-360, 338-347	50	Dagger	4	2-fold	1	-0.6	4.85	0.9	6	cryoEM	3.3	Recombinant	-18.8	-0.38	6n3a
TDP43 LC (311-360) fast sym	312-347	36	Dagger	2	2-fold screw	1	-2.8	4.75	1.0	13	cryoEM	3.8	Recombinant	-17.1	-0.47	6n37
TDP43 LC (311-360) fast asym	312-352, 311-346	41	Dagger	2	asymm. pair	n	-2.3	4.81	0.9	8	cryoEM	3.8	Recombinant	-17.6	-0.49	6n3b
TDP43 LC (267-414)	276-414	139	Meander	1	asymmetric	n	-1.7	4.73			cryoEM	3.2	Recombinant	-51.7	-0.37	7kwz
TDP43(247-257)	247-257	11	"L", straight, & curved	27	3-fold screw	n	-1.2	4.80	0.2	12	cryoEM	3.7	Synthetic	-10.7	-0.97	5w7v
Transthyretin	11-35, 57-123	92	Spearhead	1	single	n	-1.2	4.83	1.3	3	cryoEM	3.0	Human heart	-62.1	-0.68	6sdz
<b>Functional Amyloid Proteins</b>																
FUS LC domain (1-214)	37-97	61	"S", highly kinked	1	single	0	0.0	4.89	1.2	4	ssNMR	2.7	Recombinant	-12.2	-0.20	5w3n
FUS LC domain (111-214)	112-150	39	"U"	2	2-fold screw	1	-2.1	4.88			cryoEM	2.6	Recombinant	-7.3	-0.19	6xfm
FUS LC domain SYSGYS	37-42	6	Kinked	2	2-fold screw	1	0.0	4.82	0.2	2	X-ray	1.1	Synthetic	-3.6	-0.30	6bwz
FUS LC domain SYSSYGQS	54-61	8	Kinked	2	2-fold screw	1	0.0	4.79	0.8	8	X-ray	1.1	Synthetic	-3.6	-0.22	6bxv
FUS LC domain STGGYG	77-82	6	Kinked	2	2-fold screw	4	0.0	4.93	0.6	13	X-ray	1.1	Synthetic	-5.0	-0.41	6bzb
NUP98 LCD GFGNFGTS	116-123	8	Kinked	2	2-fold screw	1	0.0	4.79	0.6	14	crystal	0.9	Synthetic	-9.4	-0.59	6bzm
glucagon	1-29	29	Straight, antiparallel	2	2-fold screw	8	-2.2	9.64	0.4	8	ssNMR	1.5	Synthetic	-5.0	-0.17	6nzn
hnRNPA1 LCD GYNGFG	243-248	6	Kinked	2	2-fold screw	1	0.0	4.77	0.3	17	crystal	1.1	Synthetic	-6.3	-0.52	6bxx
hnRNPA1	251-294	45	"S"	2	2-fold screw	1	-1.9	4.74			cryoEM	2.8	Recombinant	-23.2	-0.52	7bx7
hnRNPA2	263-319	57	Kinked	1	single	1	-2.9	4.81			cryoEM	3.1	Recombinant	-21.4	-0.38	6wgk
HET-s(218-289)	224-283	60	$\beta$ -helix, 2-turn solenoid	1	single $\beta$ -helix	0	-8.0	9.48	2.8	12	ssNMR	1.5	Recombinant	-18.8	-0.30	2znm
Orb2	276-206	31	"U"	3	3-fold	0	-1.6	4.75			cryoEM	2.6	Fly brain	+0.8	+0.03	6vps
RIPK1-RIPK3	448-462, 532-549	33	"S"	2	2-fold screw	1	-4.8	10.1	0.6	4	ssNMR	poor	Recombinant	-5.7	-0.35	5v7z
$\beta$ -endorphin	1-31	31	"U"	1	Single	n					ssNMR		Recombinant	-16.8	-0.54	6tub

% Symmetry Classes are defined in Eisenberg, D. S. & Sawaya, M. R. Structural Studies of Amyloid Proteins at the Molecular Level. *Annu. Rev. Biochem.* **86**, 69–95 (2017).

<sup>§</sup> Negative values indicate left handed twists. Positive values indicate right handed twists.

\* Average RMSD over all pairwise superimpositions of N models, using only non-hydrogen atoms of the centermost chain of the fibril assembly.

# The NMR restraints were of such good quality that only a single model was reported.

@ See comment of Wälti et al. 2016, page E4981.

& Planes are least-squares fitted to alpha carbon atom positions of a chain. RMS deviations are reported from this plane, estimating warpedness. Planes are within 20° of normal to the fibril axis with rare exceptions.

^References to screw axes are actually pseudo screw axis.

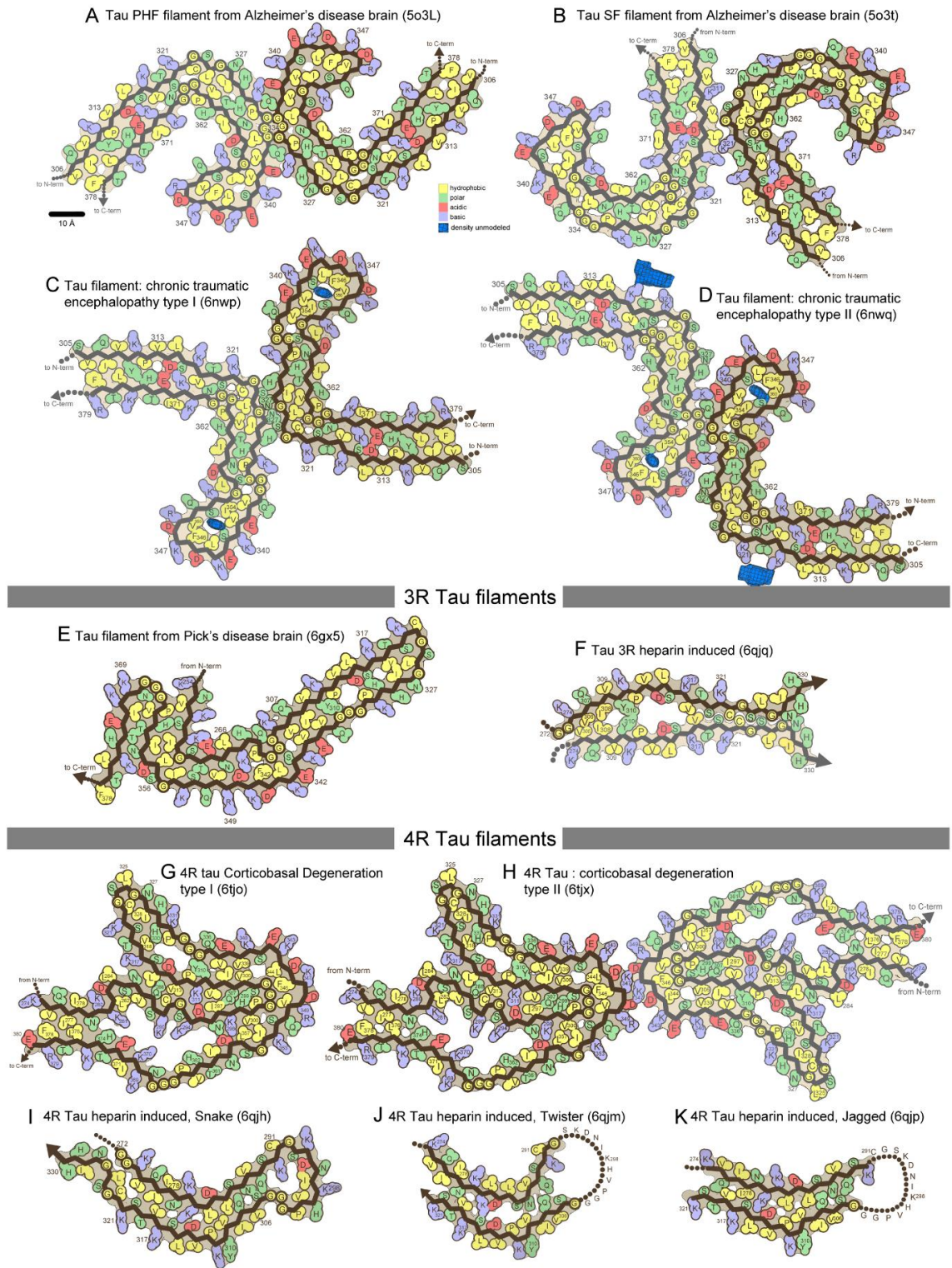
Supplementary Table 2. Notable Examples of Frustrated Regions and Their Alleviation

fibril	PDB ID code	Backbone torsional frustration		Charge Frustration				Cavities/ Channels	
		Strain	Relief	Adjacent ladders of like-charge		Ladders of uncompensated charge		Strain	relief
				Strain	Relief	Strain	Relief		
A $\beta$ (1-42)	5kk3	F19-F20-A21-D22-E23	A21G, E22G, E22 $\Delta$ , D23N	E22, D23	E22Q, E22G, E22K, E22 $\Delta$ , D23N				
transthyretin	6sdz	V16-V17, L110-L111		E66				Near K70 & K80	
$\beta$ -2-microglobulin	6gk3	L64-L65							
Islet amyloid polypeptide	6vw2	S19-S20	S20G						
antibody light chain $\lambda$ 6	6hud	A35-I36							
antibody light chain $\lambda$ 1	6ic3					E82		Three cavities: A, B, & C.	Apolar ligand in cavity C, near Ile20
serum amyloid A, mouse	6dso	M16-W17, T21-D22							
serum amyloid A, human	6mst	A27-N28				D43		Near D43	
$\alpha$ -synuclein in vitro	6h6b			K43, K45, K58	phosphate	E61		Between A56 & G73	
$\alpha$ -synuclein ex vivo, MSA case 2	6xyp			K43, K45, K58; K32, K34; K58, K60	Unknown ligands, presumably anionic	E61		Near K43, K45, K58	Unknown ligand, presumably anionic
$\alpha$ -synuclein Y39-PO <sub>4</sub> , in vitro	6l1t, 6l1u			K21, K32, K34, K43	Y39 phosphorylation			K21, K32, K34, K43	Y39 Phosphorylation
tau straight filament, Alzheimer's	5o3t, 6vi3			K321	K321 ubiquitination				
tau CBD patient brain	6tjo, 6tjx			K290, K294, K370	Unknown ligand, presumably anionic			K290, K294, K370	Unknown ligand, presumably anionic
tau Pick's Disease patient brain	6gx5							Between P312 & P332	
tau CTE patient brain	6nwp, 6nwq							Near V339, L344, F346, V350, I354	Unknown ligand, presumably aliphatic
Tau paired helical filament, Alzheimer's	5o3l, 6vhl			K317, K321	K321 ubiquitination				
$\beta$ -endorphin	6tub					E8	Low pH		
Glucagon	6nzn					D9, D15, D21	Low pH		

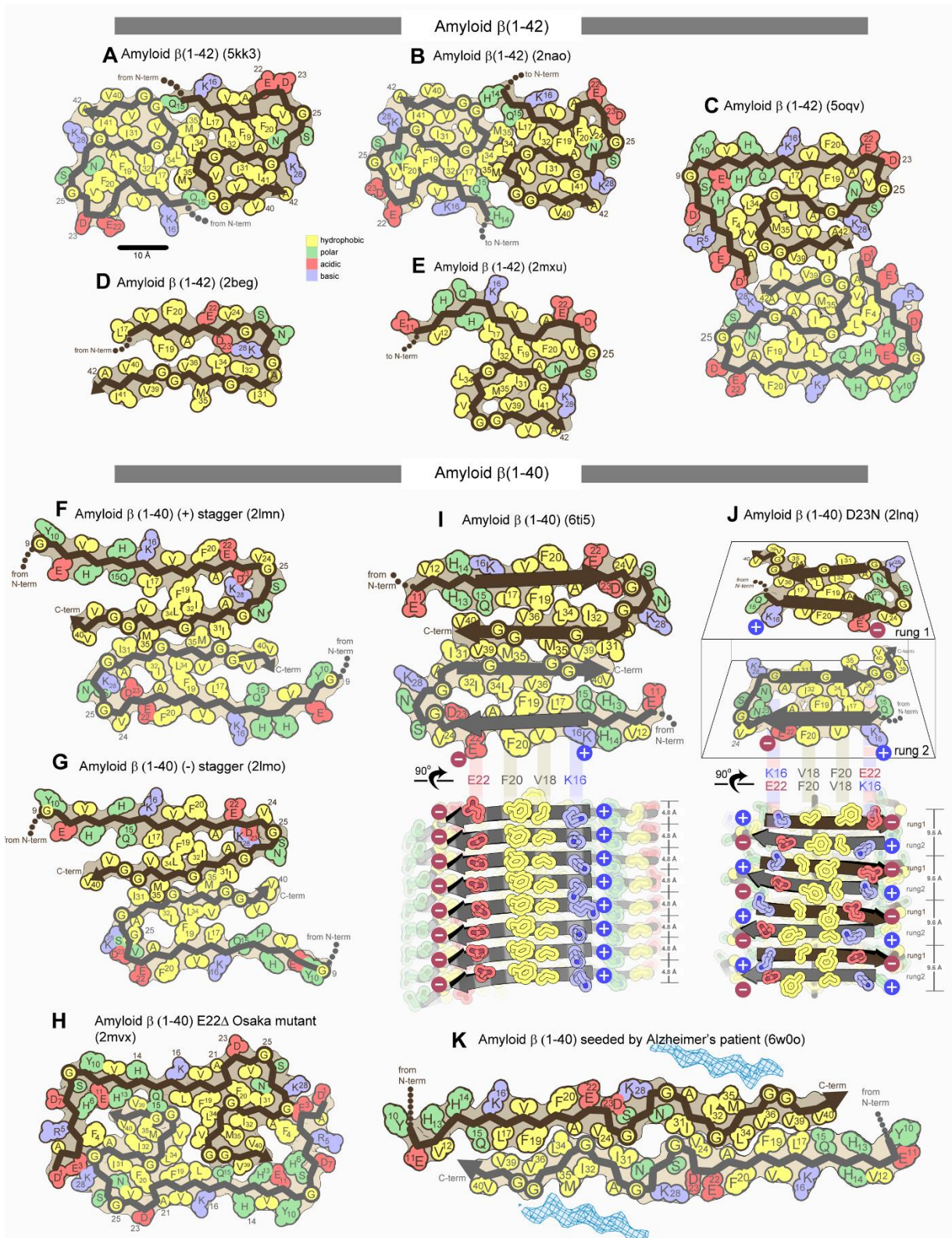
Supplementary Table 3. Functional amyloids

Class	Protein name	Function	Organism	Means of regulating assembly	Means of initiating disassembly	Fibril lifespan estimate	PDB ID code
(i) Structural	PMEL17	Template for melanin synthesis	Human	Alternative splicing of PMEL17(Dean and Lee, 2020) . Processing by compartmentalized proprotein convertase(Berson et al., 2003).	Increase pH from 4 to 7(McGlinchey and Lee, 2017)	Lifetime of cell	
	Curli	Biofilm support	<i>Escherichia and Salmonella</i>	Dedicated chaperone and nucleator proteins CsgB, CsgE, CsgF(Chapman et al., 2002)	None	Beyond lifetime of cell	
	Chaplins	Assist hyphae formation by modulating surface tension	<i>Streptomyces</i>	Chaplins have a sorting signal that targets them to the cell wall or secretion(Claessen et al., 2003)	None	Beyond lifetime of cell	
	Hydrophobins	Assist hyphae formation by modulating surface tension	<i>Neurospora crassa</i>	Monomers are secreted to hydrophobic-hydrophilic interface to initiate assembly.(Macindoe et al., 2012)	None. Disassembly requires treatment with strong acid.	Beyond lifetime of cell	
(ii) Storage	$\beta$ -endorphin	Regulates stress response and pain perception.	human	Concentration in secretory granule at pH 5.5(Maji et al., 2009).	Release into blood with pH increase to 7(Maji et al., 2009)(Nespovitaya et al., 2016)	Less than lifetime of cell.	6tub
	Glucagon	Regulates the conversion of glycogen to glucose	Human	Fibrils nucleate upon pH drop, enabling storage in secretory granules(Maji et al., 2009).	Not known.	Less than lifetime of cell.	6zn
	FUS, hnRNP1, hnRNP2, etc.	Formation of stress granules, suppression of transcription during stress	human	Induced by stress.	Karyopherin- $\beta$ 2 binds the nuclear localization sequence(Guo et al., 2018).	Less than lifetime of cell.	5w3n
(iii) Information carrier	HET-s prion	Immune system, signal heterokaryon incompatibility	<i>Podospora anserina</i>	Species-specific machinery not required(Taneja et al., 2007).	Perhaps chaperones like GroEL(Wälti et al., 2017)	Beyond lifetime of cell.	2nm
	Sup35, New1P, etc.	Produce cryptic genetic variation in times of stress(Tuite and Serio, 2010)	<i>Saccharomyces cerevisiae</i>	Aggregation of other prions like Rnq1(Tuite and Serio, 2010) and PIN(Villali et al., 2020)	Chaperones like Hsp104 and Hsp70(Haslberger et al., 2010)	Beyond lifetime of cell	
	Mnemons, CPEB, Orb2	Store memories	Yeast, <i>Aplysia</i> , <i>Drosophila</i>	Transient increase in protein levels signaled by a neurotransmitter like serotonin(Si et al., 2003)	Time.		6vps
(iv) Suppression of function	Cdc19 pyruvate kinase	Stress granules	Yeast	Oligomerization and phosphorylation protect Cdc19 from aggregation. Glucose starvation and dephosphorylation of Cdc19 induce aggregation. (Saad et al., 2017)	Glucose re-supplied.	Less than lifetime of cell	
(v) Signaling	Receptor-interacting protein kinases RIPK1 and RIPK3	Signal necroptosis	Human	Phosphorylation of RIPK1 and RIPK3(Cho et al., 2009)	Ultrastable, requires 150 mM NaOH to be disassembled (Li et al., 2012).	Beyond lifetime of cell.	5v7z

Tau filaments assembled from all 6 brain isoforms

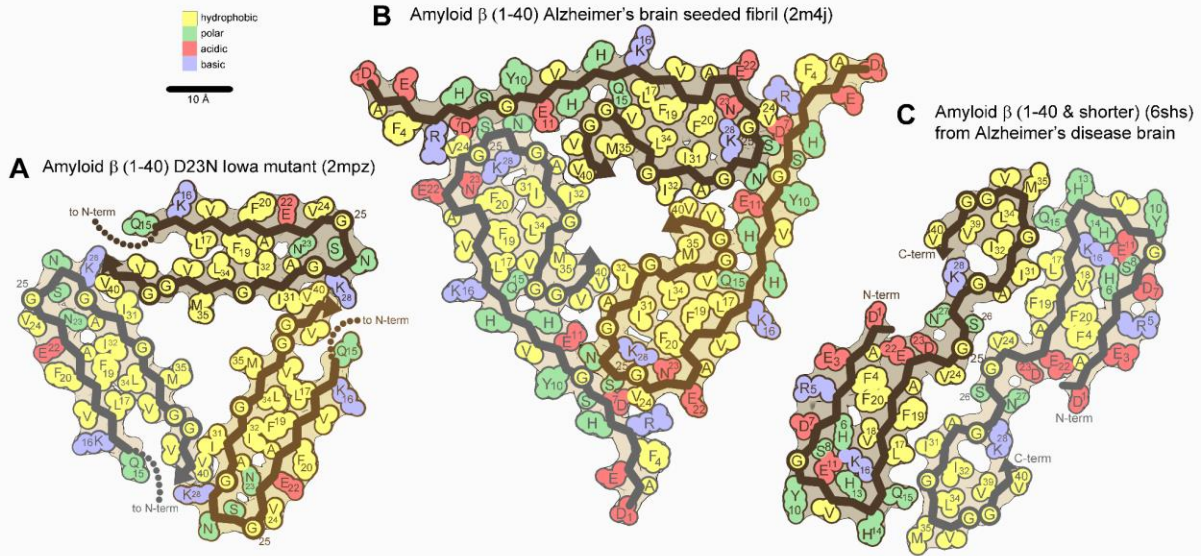


**Supplemental Figure 1. Structures of tau amyloid fibril polymorphs.** (A-D) Fibrils composed of 3R and 4R isoforms. (E-F) Fibrils composed of 3R isoforms only. (G-K) Fibrils composed of 4R isoforms only. Structures in panels A-E and G-H are from *ex vivo* fibrils. The remaining panels depict recombinant tau.

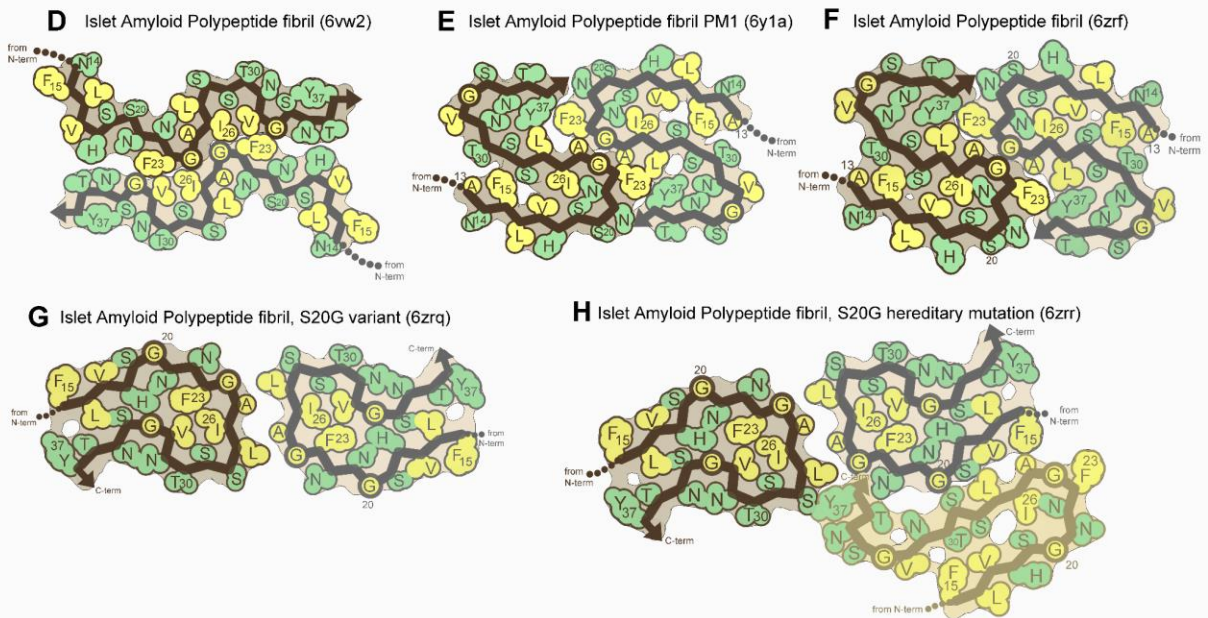


**Supplemental Figure 2. Structures of some A $\beta$  fibril polymorphs.** (A-E) 42-residue A $\beta$  isoform (F-K) 40-residue isoform of A $\beta$  (I) The parallel in-register scaffold is usual among amyloids where like-charges stack in columns. (J) A rare instance of an antiparallel  $\beta$ -sheet scaffold. Neighboring strands in the sheet run in opposite directions (brown vs. gray). Note that the antiparallel (but not the parallel) scaffold allows for charge complementation between K16 and E22.

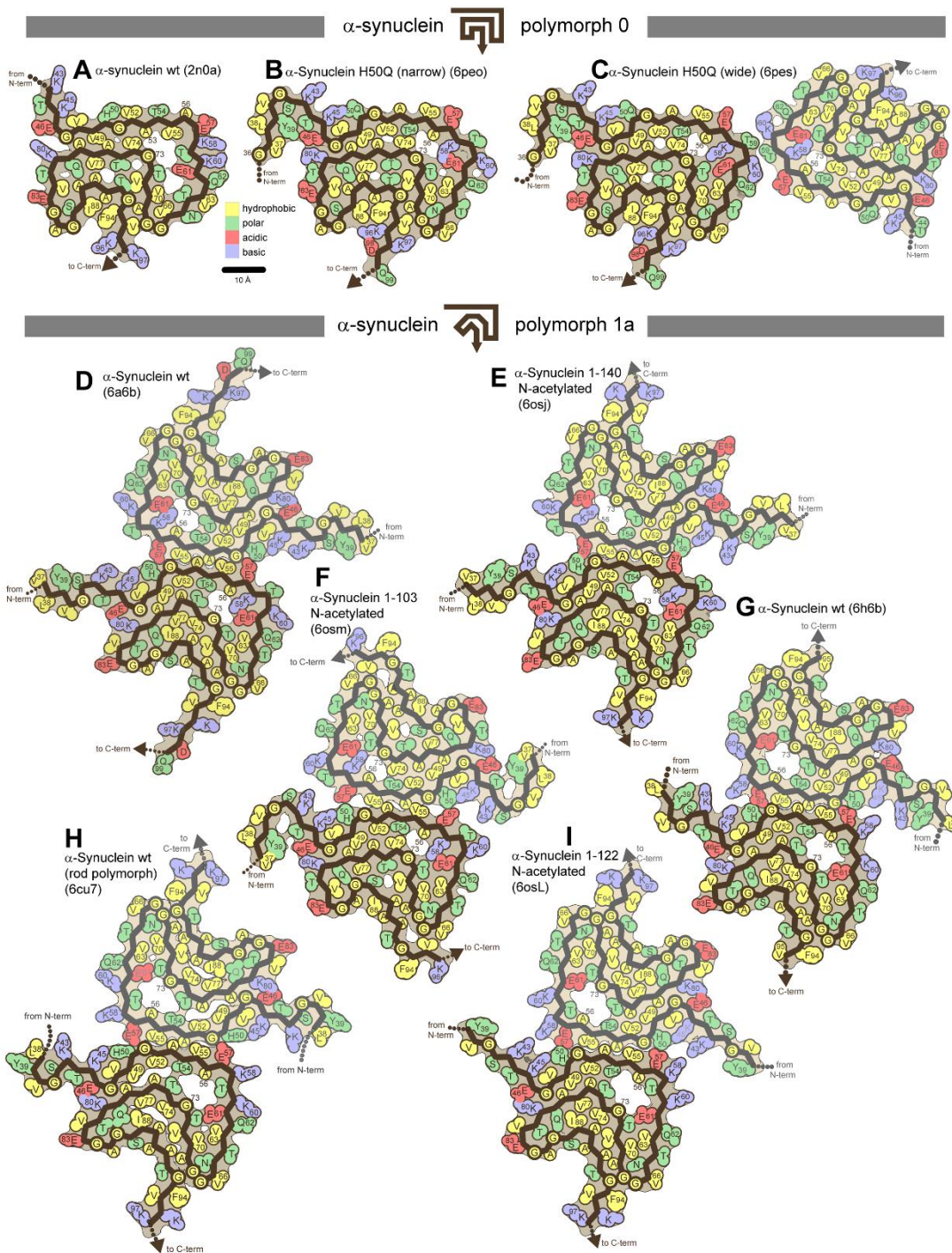
Amyloid  $\beta$ (1-40) continued



Islet Amyloid Polypeptide (IAPP)



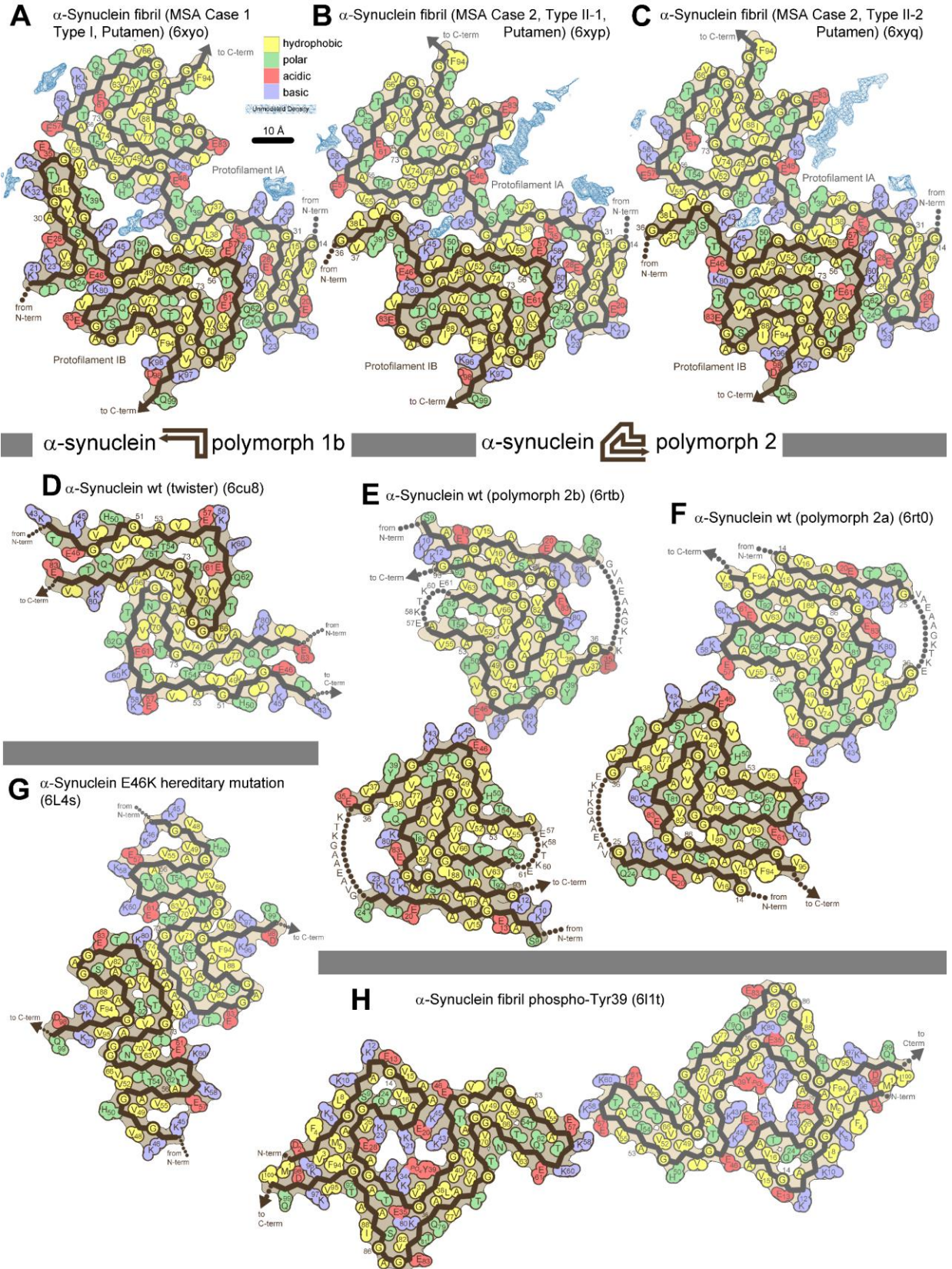
Supplemental Figure 3. Structures of  $A\beta$  fibril polymorphs (continued) and IAPP.



**Supplemental Figure 4. Structures of α-synuclein amyloid fibril polymorphs 0 and 1a.** Even among members of the same polymorph family, local differences in backbone conformations are observed and side chains such as K58 may be either inward or outward facing.

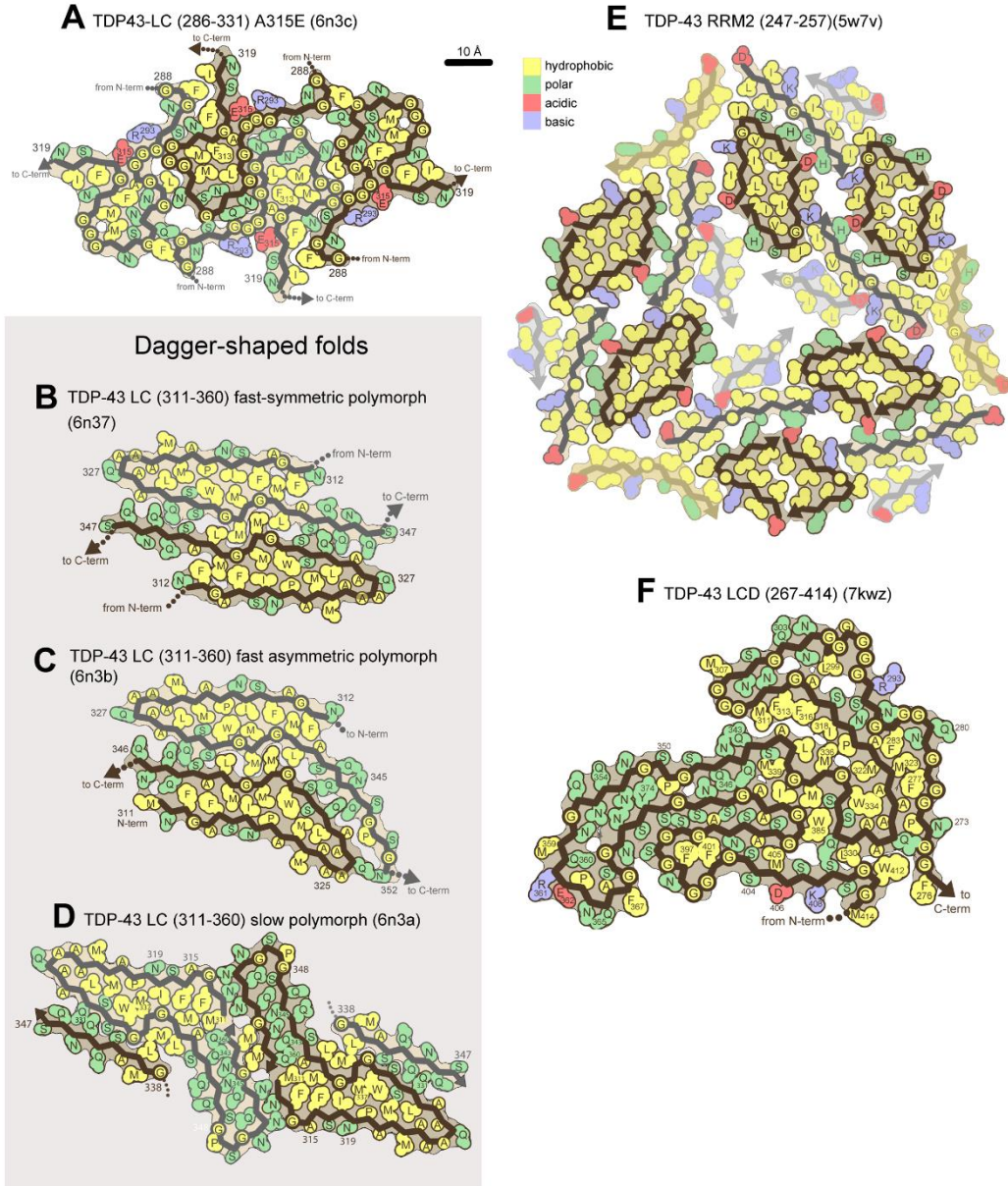


$\alpha$ -synuclein ex vivo

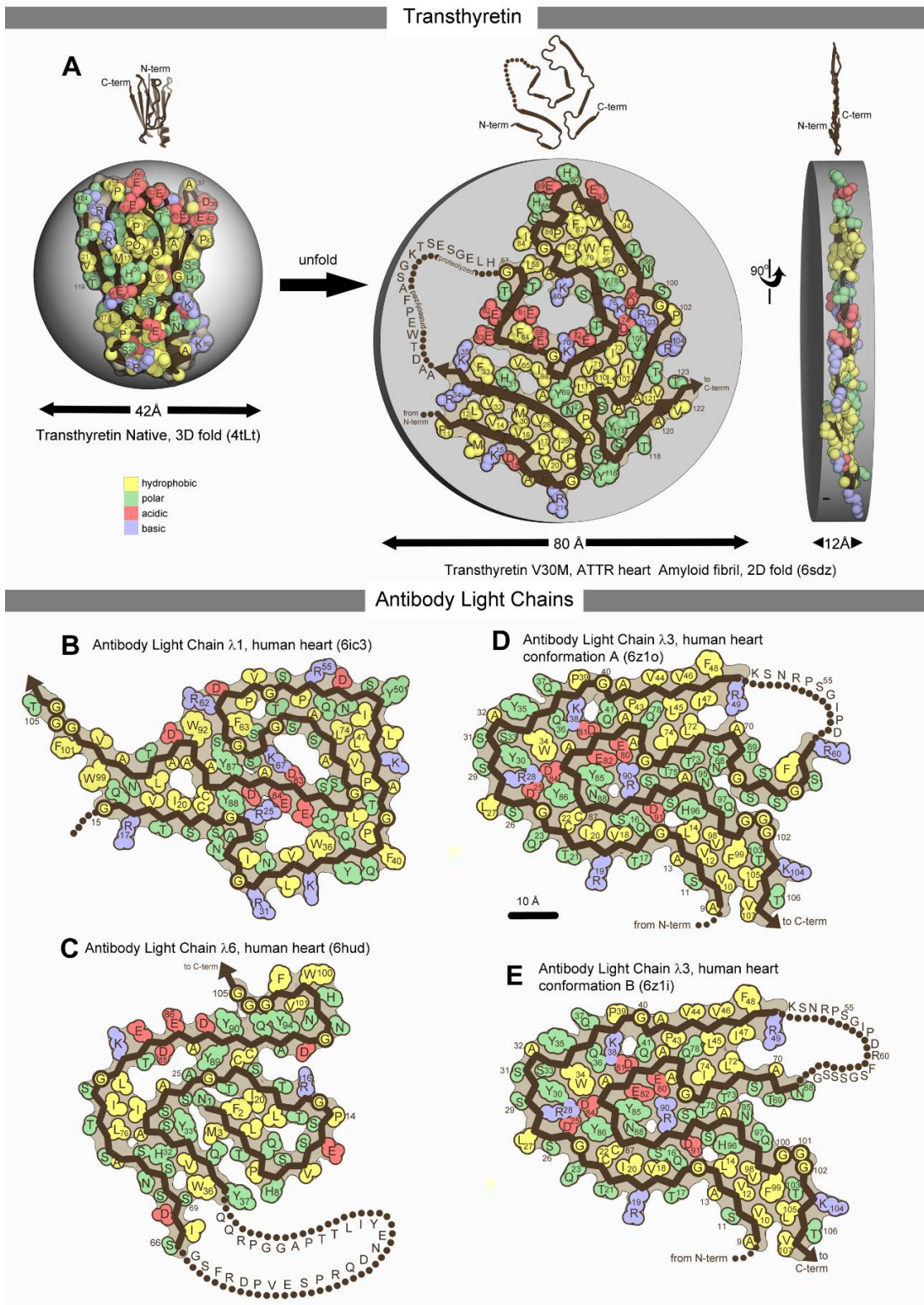


Supplemental Figure 5. Structures of  $\alpha$ -synuclein amyloid fibril polymorphs 1b, 2, and others.

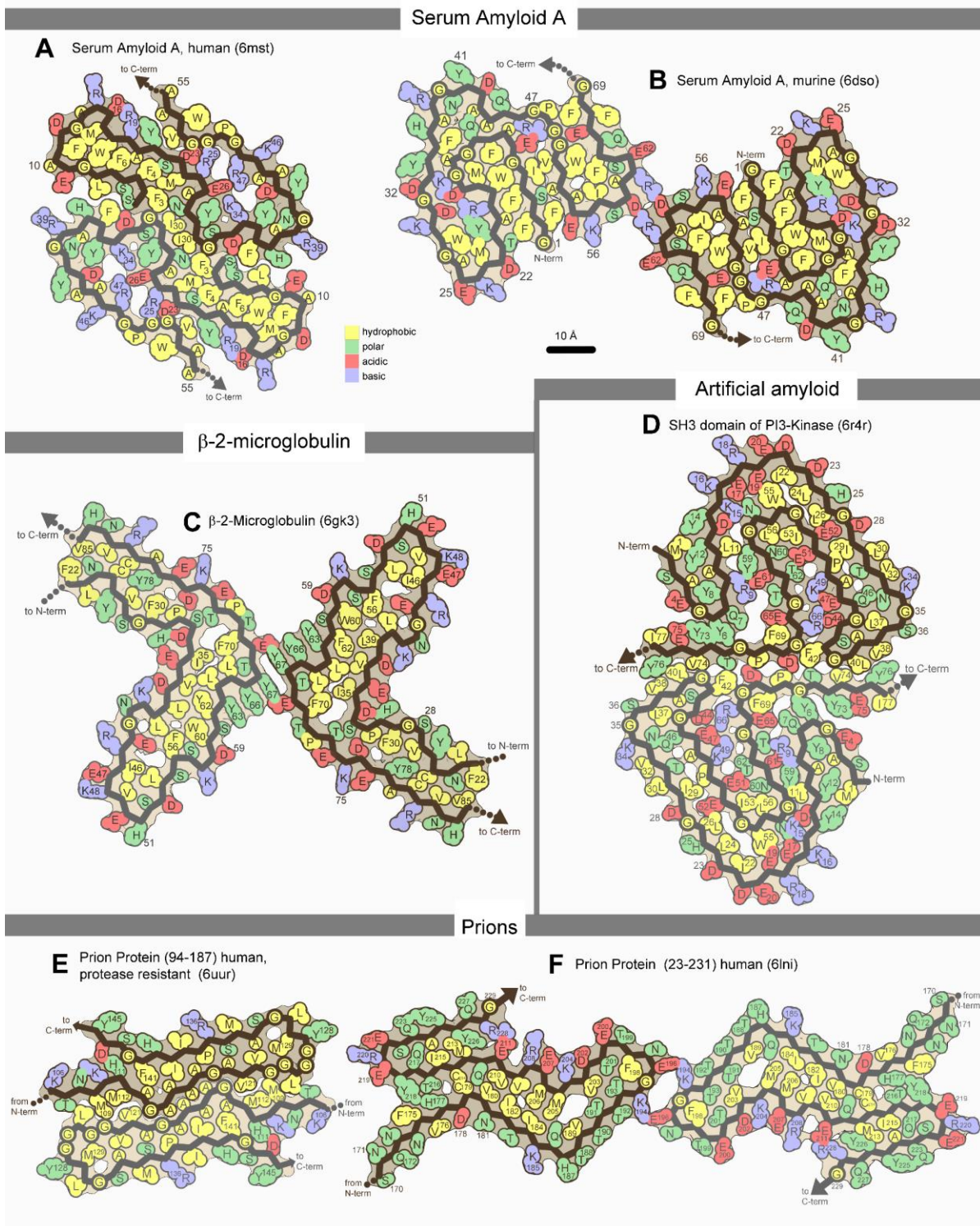
TDP-43 domains



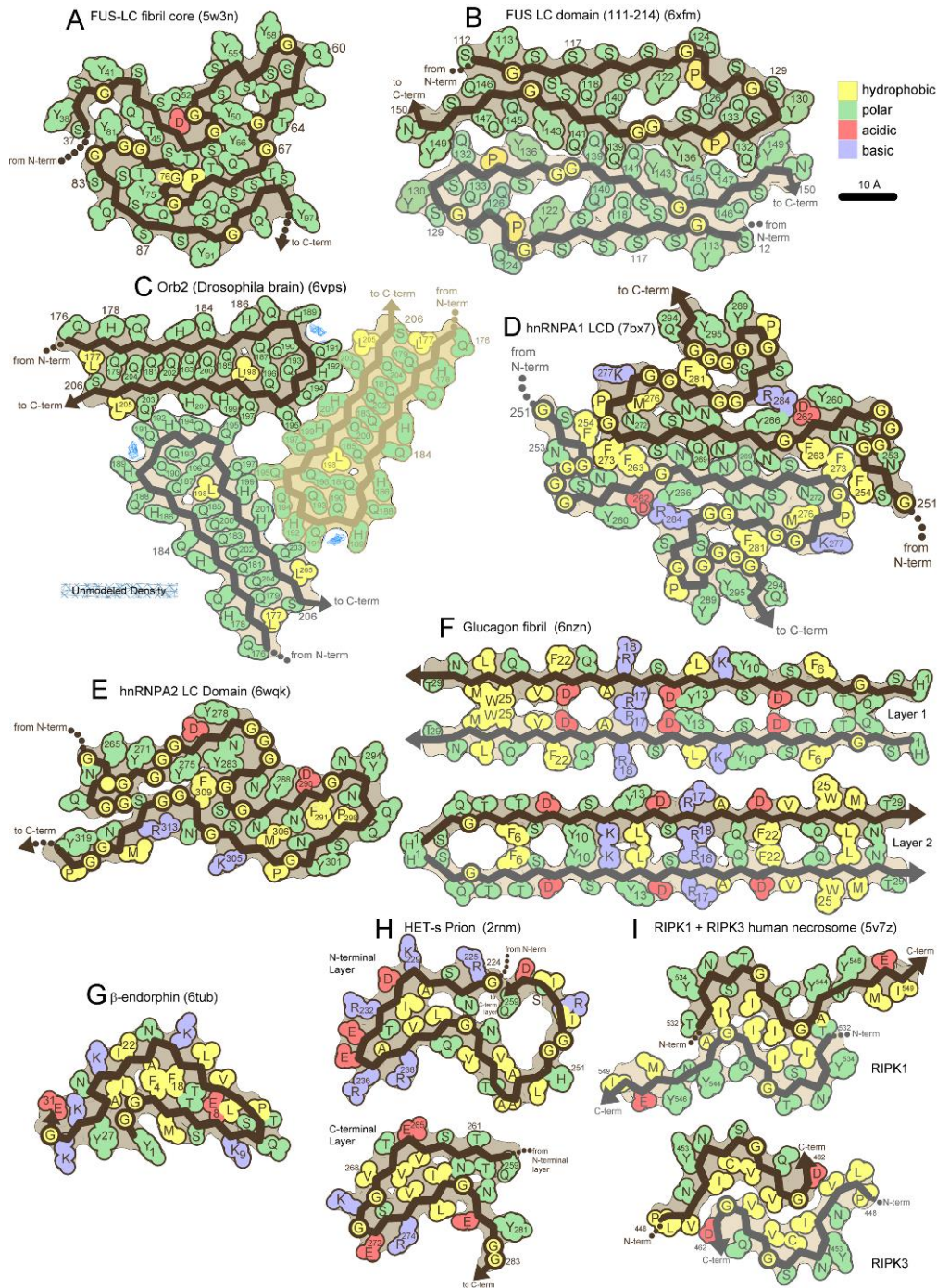
Supplemental Figure 6. Structures of TDP-43 amyloid fibrils produced with recombinant protein.



**Supplemental Figure 7. Structures of proteins involved in two systemic amyloid diseases: transthyretin amyloidosis and light chain amyloidosis.** (A) Left panel shows transthyretin in its native 3-dimensional state. The center and right panels show transthyretin in the amyloid state and highlight its confinement to a thin, nearly 2-dimensional layer. (B-D) Structures of antibody light chain amyloid fibrils extracted from patients of light chain amyloidosis.

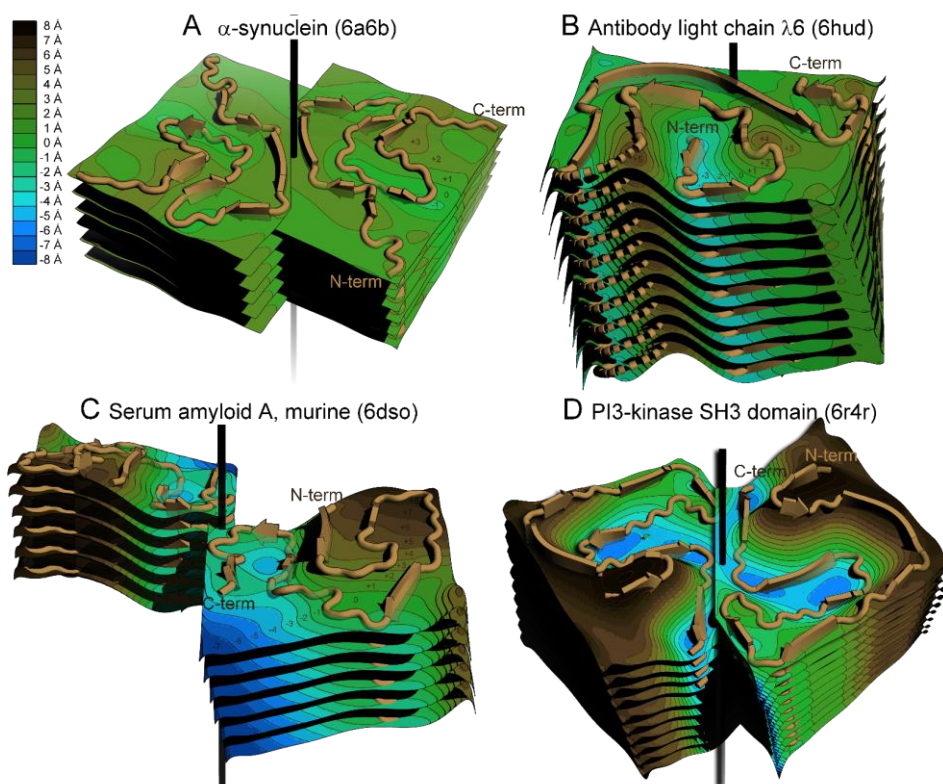


**Supplemental Figure 8. Structures of various amyloid proteins.** (A-B) Serum amyloid A fibrils extracted from AA amyloidosis patients. (C) β-2-microglobulin fibrils are associated with dialysis-related amyloidosis. This fibril was prepared from recombinant protein. (D) The SH3 domain of PI3-Kinase is not associated with disease. It is an artificially created amyloid fibril which has been the subject of extensive mutagenesis to probe the role of sequence on amyloid fibril formation and growth. (E,F) Prion fibrils prepared from recombinant protein.

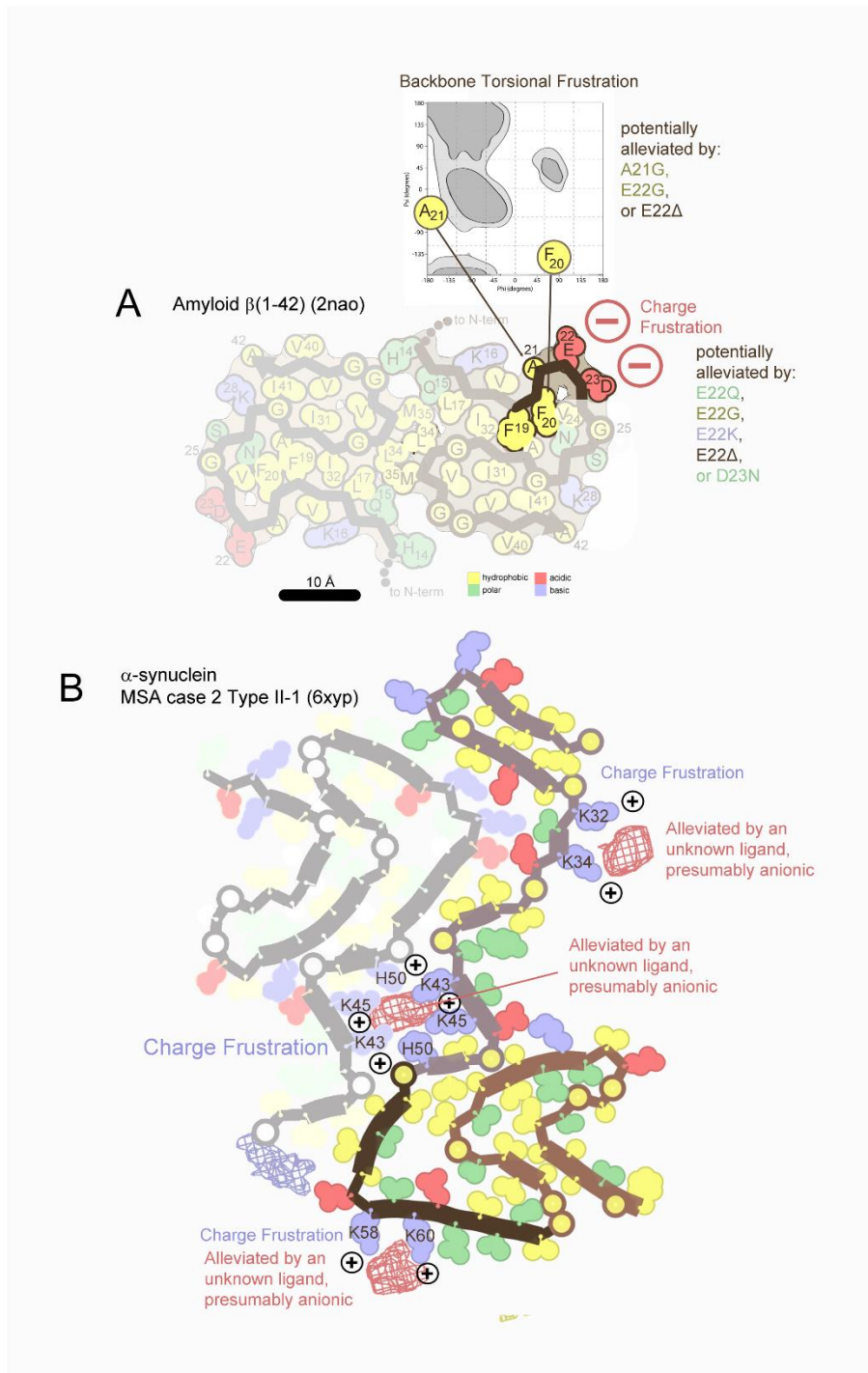


**Supplemental Figure 9.** Proteins that form functional amyloid fibrils. (A and B) FUS LCDs form hydrogels (C) Orb2 (*ex vivo*) aids memory formation (D) hnRNP1 forms a component of stress granules. The fibril depicted here is reportedly pathogenic (E) hnRNP2 also participates in stress granule formation (F) Glucagon is a hormone that regulates blood sugar concentration. Glucagon forms fibrils as a functional mechanism of hormone

storage, but its high propensity fibrilize also has medical implications. Diabetics that require a supplementary source of glucagon dissolve dry glucagon powder (at acidic pH to ensure activity) and this solution must be administered immediately. Delays of only an hour lead to the formation of nuisance fibrils, composed of antiparallel sheets. The alternating antiparallel layers, 1 and 2, are shown separately. This structure may aid in engineering a variant of glucagon that is resistant to fibril formation. (G)  $\beta$ -endorphin, (H) Het-s and (I) RIPK1-RIPK3 fibrils perform a functional role. Het-s and RIPK1-RIPK3 are either biologically irreversible or disassembled by ATP-consuming chaperone. In Het-s fibrils, successive layers alternate between N and C-terminal segments. Similarly, in RIPK1-RIPK3 fibrils, successive layers alternate between RIPK1 and RIPK3. Hence, these fibrils are represented as two distinct layers.



**Supplemental Fig. 10. Amyloid 2D folds exhibit varying degrees of warping.** Warping is defined as the deviation of amyloid protein backbone from its best fit plane. Generally, the best fit plane lies nearly perpendicular to the fibril axis. Each protein chain in this figure was fit to a 2-dimensional surface using a 10-term Maclaurin series. Parts of the chain that dip below the best-fit plane are highlighted by blue depressions and parts of the chain that rise above the best-fit plane are highlighted by brown peaks as indicated by the color gradient key on the left. Deviations from the best-fit plane are typically small (around 1.0 Å RMSD for  $\alpha$ -carbon atoms) as illustrated in Panel A, a topographical map of  $\alpha$ -synuclein (rod polymorph, 6a6b) which is nearly flat. A higher degree of warping (1.9 Å RMSD) is illustrated for antibody light chain amyloid (PDB ID 6hud) in Panel B. Here, alpha carbons deviate from -6 Å to +6 Å from the best-fit plane, giving the appearance of shallow hills and valleys. Panel C and D show examples of more extreme warping. In Serum Amyloid A (6dso) a single chain traverses 16 Å from the highest point near the N-terminus (brown) to its lowest point near the C-terminus (blue), fitting a warped plane that gently tilts ( $14^\circ$ ) away from the fibril normal. In PI3-kinase SH3 domain (6r4r) a single chain traverses about 18 Å along the fibril direction. Here, a steep cliff separates the C-terminus lying in a central depression from the N-terminus skirting a high plateau.



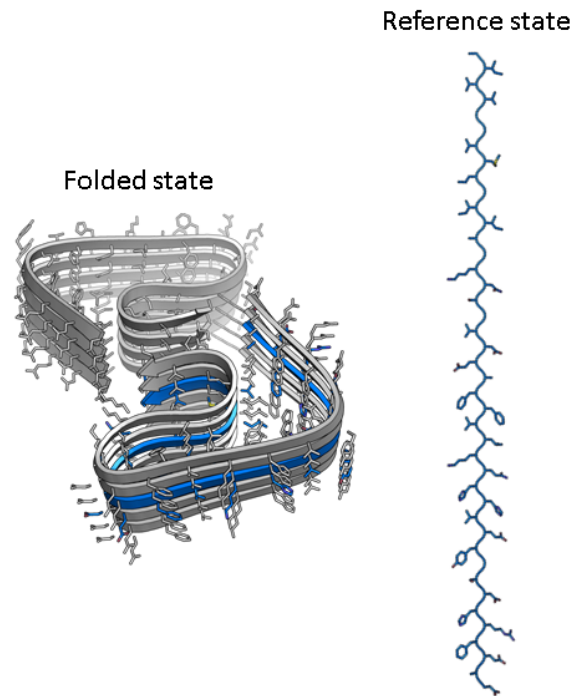
**Supplemental Figure 11. Examples of frustrations in amyloid fibrils and how they might be alleviated.** (A) Backbone torsion frustration in  $\text{A}\beta(1-42)$ , PDB ID 2nao is evident in residues F20 and A21 as Ramachandran plot outliers. This torsional frustration might be alleviated by hereditary mutations which replace residues in this region with amino acids of smaller size. Charge frustration is evident in the adjacent ladders of negative charge at E22 and D23. Charge frustration in this region might be alleviated by hereditary mutations that eliminate negative charge. The early onset of AD caused by these mutations might be explained by their ability to alleviate these frustrations in the fibril and accelerate fibril growth. (B) Charge frustrations are evident in  $\alpha$ -synuclein extracted from MSA patients, PDB ID 6xyp. Residual cryoEM density near these regions of positive charge repulsion might correspond to anions. Growth of this polymorph might depend on the availability of this unknown ligand.

- Evaluate solvent accessible surface area (SASA) of a central strand within an amyloid fibril (Folded state).
- Evaluate SASA of isolated, extended strand using an approximation (Reference state). That is, for residue  $n$ , evaluate SASA for the isolated tripeptide in the absence of side chains on  $n-1$  and  $n+1$ .
- Take the difference,  $SASA_{Ref} - SASA_{Fold}$  for each atom to get area buried.
- Multiply the area buried by the Atomic Solvation Parameter (ASP).

+18 cal/mol/Å<sup>2</sup> for C  
 -5 cal/mol/Å<sup>2</sup> for S  
 -9 cal/mol/Å<sup>2</sup> for N,O uncharged  
 -38, -37 cal/mol/Å<sup>2</sup> for N,O charged

Except in the following cases:

1. ASP=0 for **Asn** or **Gln** side chains N and O elements with two-H-bonds and less than 5 Å<sup>2</sup> SASA.
  2. ASP=0 for backbone N and O elements involved in a H-bond.
  3. ASP>-9 for ionizable N or O elements involved in ion pair and less than 50 Å<sup>2</sup> SASA. Ion pair distance must be less than 4.5 Å. ASP depends on distance as follows: A.S.P. = -9 \* ((dist-2.8Å)/2.8Å)<sup>2</sup>.
  4. Include entropy terms from Koehl & Delarue 1994 scaled by percentage of side chain surface area buried.
- Sum up the energies of all the atoms to get the solvation energy. Negate this value to get stabilization energy.
  - Less sensitive to structural errors than Rosetta.



Eisenberg D, Wesson M, Yamashita M (1989) Interpretation of protein folding and binding with atomic solvation parameters. *Chemica Scripta* 29A: 217–221.  
 Koehl P, Delarue M. Application of a self-consistent mean field theory to predict protein side-chains conformation and estimate their conformational entropy. *J Mol Biol.* 1994 Jun 3; 239(2):249-75.

**Supplemental Figure 12. Some details of calculation of solvation energies of stabilization of amyloid fibrils.** The standard free energy of stabilization of a given amyloid chain is computed as the difference in atomic solvation energy of the exposed, solvated chain and the folded chain in the center of five layers of the known structure of a protofilament. The atomic solvation parameters are augmented with terms to describe the entropy change of sidechains upon folding, scaled by the percentage of side chain surface area buried. Current energy evaluations are helpful but incomplete guides to predict lifespans of fibrils.